Textural identification of carbonate rocks by image processing and neural network: Methodology proposal and examples

Article *in* Computers & Geosciences · June 2005

DOI: 10.1016/j.cageo.2004.11.016

CITATIONS
72

READS
1,331

5 authors, including:

Roberto Marmo
University of Pavia
26 PUBLICATIONS **131** CITATIONS
SEE PROFILE

Sabrina Amodio
Parthenope University of Naples
39 PUBLICATIONS **537** CITATIONS
SEE PROFILE

Roberto Tagliaferri
Università degli Studi di Salerno
285 PUBLICATIONS **3,130** CITATIONS
SEE PROFILE

Giuseppe Longo
University of Naples Federico II
425 PUBLICATIONS **5,865** CITATIONS
SEE PROFILE

ELSEVIER

Computers & Geosciences 31 (2005) 649–659

COMPUTERS & GEOSCIENCES

www.elsevier.com/locate/cageo

Textural identification of carbonate rocks by image processing and neural network: Methodology proposal and examples ☆

Roberto Marmo[a,*], Sabrina Amodio[b,c], Roberto Tagliaferri[d,e], Vittoria Ferreri[b], Giuseppe Longo[f,g]

[a]*Dipartimento di Informatica e Sistemistica, Università di Pavia, Via Ferrata 1, 27100 Pavia, Italy*
[b]*Dipartimento di Scienze della Terra, Università Federico II, Largo San Marcellino 10, 80138 Napoli, Italy*
[c]*Istituto per l'Ambiente Marino Costiero (IAMC), Geomare. National Research Council, Calata Porta Di Massa, Porto di Napoli, 80133 Napoli, Italy*
[d]*Istituto Nazionale Fisica della Materia, unità di Salerno, 84081 Baronissi (Sa), Italy*
[e]*Dipartimento Matematica e Informatica, Università di Salerno, via S. Allende, 84081 Baronissi (Sa), Italy*
[f]*Dipartimento di Scienze Fisiche, Università Federico II di Napoli, Polo della Scienza e della Tecnologia, via Cinthia 9, 80133 Napoli, Italy*
[g]*Istituto Nazionale di Fisica Nucleare, sezione di Napoli, 80133 Napoli, Italy*

Received 26 November 2004; accepted 26 November 2004

Abstract

Using more than 1000 thin section photos of ancient (Phanerozoic) carbonates from different marine environments (pelagic to shallow-water) a new numerical methodology, based on digitized images of thin sections, is proposed here. In accordance with the Dunham classification, it allows the user to automatically identify carbonate textures unaffected by post-depositional modifications (recrystallization, dolomitization, meteoric dissolution and so on). The methodology uses, as input, 256 grey-tone digital image and by image processing gives, as output, a set of 23 values of numerical features measured on the whole image including the "white areas" (calcite cement). A multi-layer perceptron neural network takes as input this features and gives, as output, the estimated class. We used 532 images of thin sections to train the neural network, whereas to test the methodology we used 268 images taken from the same photo collection and 215 images from San Lorenzello carbonate sequence (Matese Mountains, southern Italy), Early Cretaceous in age. This technique has shown 93.3% and 93.5% of accuracy to classify automatically textures of carbonate rocks using digitized images on the 268 and 215 test sets, respectively. Therefore, the proposed methodology is a further promising application to the geosciences allowing carbonate textures of many thin sections to be identified in a rapid and accurate way.

A MATLAB-based computer code has been developed for the processing and display of images.

Keywords: Carbonate rocks; Thin sections; Dunham classification; Multi-layer perceptron; Image analysis

☆ Code on server at http://www.iamg.org/CGEditor/index.htm.

*Corresponding author. Tel.: +39 382 505486; fax: +39 382 505373.
E-mail addresses: marmo@vision.unipv.it (R. Marmo), sabrina.amodio@iamc.cnr.it (S. Amodio), robtag@unisa.it (R. Tagliaferri).

0098-3004/$ - see front matter © 2005 Elsevier Ltd. All rights reserved.
doi:10.1016/j.cageo.2004.11.016

1. Introduction

The texture classification is the first step to identify the lithofacies of the sedimentary rocks to recognize their original depositional environment. A texture is individuated by visual estimation in the field with a hand lens of $\cong 10\times$ as well as in thin section. In sedimentology the most widely used and simplest texture classification of carbonate rocks is that of Dunham (1962), because it is only based on sediment fabric. Limestones are divided into three main textural groups (Tucker and Wright, 1990): mud-supported (mudstones and wackestones), grain-supported (packstones and grainstones) and biologically bounded together during deposition (boundstones); the last category is not considered in this paper. Mudstones and wackestones contain less and more than 10% grains, respectively. Mud is still present in packstones which are grain-supported while is totally lacking in grainstones. The Dunham classification provides a clue to the environmental energy during deposition. For example, a mudstone reflects low-energy conditions on the contrary of a grainstone.

Note that the term texture in image processing is generally used to describe the repetition of basic elements (texel) for the characterization of given object-surfaces. In this paper, instead, by texture we refer to the space-organization of the main constituents of a sedimentary rock: grains, matrix (depositional components) and cement (post-depositional precipitate in the pore space), as customary in sedimentology and sedimentary petrology.

A recent application of neural networks uses composite well-data to provide petrophysical information (Chang et al., 2002). Further neural networks applications to geosciences can be found in Tagliaferri et al. (2003).

Hereafter, we propose a new methodology to identify automatically textures of Phanerozoic marine carbonate rocks in thin section by image processing and neural networks. This is a pilot study which allows the proposed model to be tested on all types of carbonates. In perspective, this technique represents a potentially interesting approach for petroleum geologists to rapidly analyze many thin sections.

2. Methodology

In order to classify the texture of a carbonate rock from a thin section, it is necessary to distinguish skeletal (organism-derived) and non-skeletal (mostly biochemical precipitates) grains, as well as matrix and sparry calcite cement. Grains are largely biogenic fragments (marine invertebrates and algae) or whole fossils. The main problem is that the unit of information in a digitized image is the pixel and each pixel has properties of position and grey value; however, by itself, the knowledge of the position and value of a particular pixel does not generally convey any geological information related to the recognition of a texture. To avoid this problem an alternative set of features is needed.

The image processing techniques allow to extract from an image a set of numerical features, expressed as coded characteristics of the selected object, and used to differentiate one class of objects from another.

The neural networks classify a thin section texture after training on a specific data set by taking into account all extracted features, or a part of them. Each output of the neural network is the probability to classify an input section belonging to a specific Dunham class. We assign the input section to the class associated with the highest value to the output.

The main steps of this methodology (Fig. 1), applied to each image of thin section, are

a. image acquisition;
b. image filtering;
c. feature extraction;
d. feature normalization;
e. input dimension reduction;
f. neural network.

The image processing is related to techniques at points (a)–(c). Gonzalez (2004) and Shapiro and Haralick (1993) describe the mathematical details related to them. In the following sections we explain the details of these techniques.

This methodology is implemented in MatLab® (The MathWorks Inc.) code and toolbox: Image Processing, Netlab (Nabney, 2002). The codes have been written as part of a package, which can be used and extended for future applications. The software performs the classification on a digitized image in few seconds, using a desktop computer based on Intel® Pentium IV and Windows XP® operating system.

2.1. Image acquisition

Image acquisition describes the process of converting a picture into its numerical representation, which is suitable for further image processing steps. The acquisition process is physically accomplished by a digitizer.

With digital image we refer to a two-dimensional matrix M, each $M(i,j)$ is a pixel at row i and column j that contains the grey tone related to real image.

This methodology requires bitmap images with 8-bit 256 linear grey tones (0 corresponds to black colour and 255 to the white one) with dimensions of 700×500 pixels acquired by a digital camera with 150 dots per inch. The magnification was about 20–25$\times$ to optimize the acquisition of smaller and larger (skeletal and non-skeletal) grains.

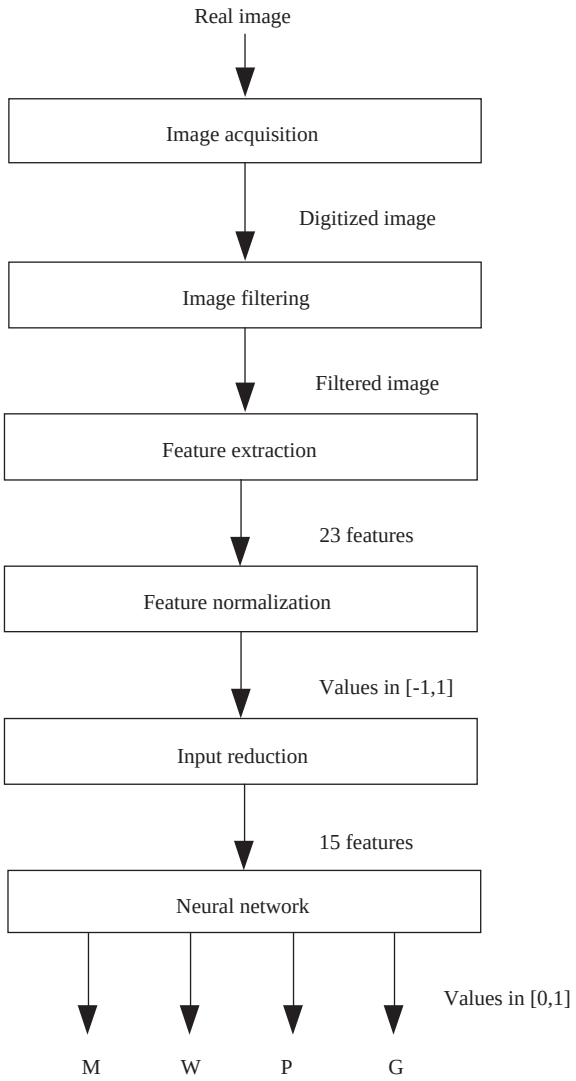

Fig. 1. Main phases of proposed methodology.

To get a homogeneous data base, all images were acquired in grey scale because only a little portion was originally in colour. Moreover, this methodology contemplates only the shape of white areas due to cement and of grey areas ascribed to matrix and grains.

Before the acquisition, brightness and contrast of all images have been adjusted, for a better stand out of the grains from the matrix or cement background.

2.2. Image filtering

Due to high quality of images, the median filter and a neighbourhood of 3×3 pixels are sufficient to remove small distortions without reducing the sharpness of the image.

2.3. Feature extraction

This step is composed of a sequence of operations on image matrix, in order to measure the features of the objects. These values are given as input to the neural network.

We have performed several tests on different types of features. The final set is composed of the following 23 features:

1. percentage of the most frequent grey tones;
2. number of edge pixels in the grey areas;
3. number of edge pixels between the grey and the white areas;
4. number of white areas;
5. number of pixels of white areas;
6. number of white areas composed of more than 150 pixels;
7. number of pixels within the white areas composed of more than 150 pixels;

   7 features (1)–(7) were extracted from the whole image and the remaining 16 features were extracted from each of the 4 selected largest white areas (4 features (8)–(11) per area):
8. number of pixels of the white area;
9. length in pixel of the white area;
10. number of small convex deficiencies;
11. number of large convex deficiencies.

Each of the above features is described in the following sections.

2.3.1. Percentage of the most frequent grey tone

An image histogram is a chart that shows the frequency of the grey tones. This plot is composed of 20 equally spaced bins, each representing a range of grey tone. It is necessary to sum the number of pixels of the bins chosen around the bin that corresponds to the most frequent grey tone. The value of this feature is the ratio between this sum and the sum of the pixels in all the bins. An image of a grainstone (Fig. 2) has a large and broader histogram (Fig. 3) because it is composed of many pixels distributed on many grey tones. Instead, an image of a mudstone has a narrower and higher histogram, because a mudstone, being very fine grained, is represented by many pixels distributed on few grey tones.

2.3.2. Number of edge pixels in the grey areas

To find edges in the whole image, the Canny operator looks for places where the intensity changes rapidly. The resulting image is a black/white image in which a black pixel corresponds to an edge pixel in the original image. We chose this operator because it is more likely to detect weak edges. The low and high thresholds are 0.25 and

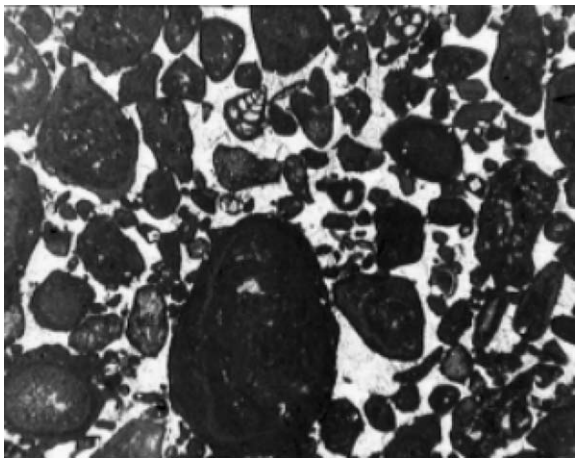

Fig. 2. Example of grainstone texture with intergranular sparry calcite cement.

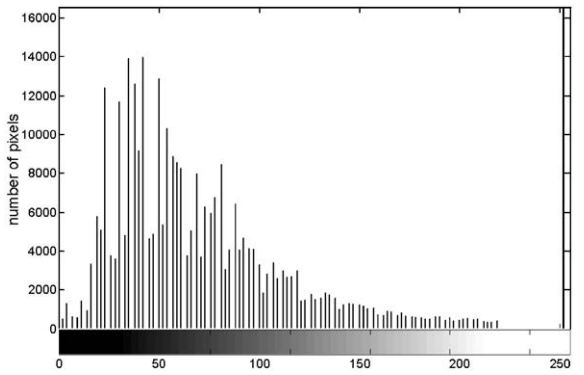

Fig. 3. Larger and broader image histogram related to thin section of Fig. 2. In lower part, colour map of 256 8-bit grey tones is shown.

1.00. The value of the feature is the number of black pixels. The resulting image of a grainstone has many black pixels (Fig. 4) because, being a grain-supported texture, it is composed of numerous skeletal and non-skeletal grains that create a large number of edges. On the contrary, a mudstone has few black pixels because it is composed of large homogeneous, very fine grained, hardened mud.

2.3.3. Number of edge pixels between the grey and the white areas

A pixel is considered as a perimeter pixel if it satisfies both the following criteria: it is a white pixel in the starting image and shows one or more grey pixels in its 8×8 neighbourhood. The value of the feature is the number of perimeter pixels. The white areas are due to crystals of sparry calcite cement, filling the inter-

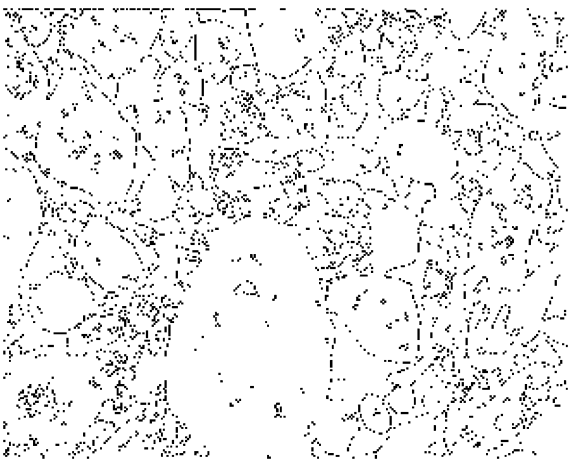

Fig. 4. Resulting image of Canny operator related to thin section of Fig. 2. Each black pixel corresponds to an edge between grey areas or between white and grey areas.

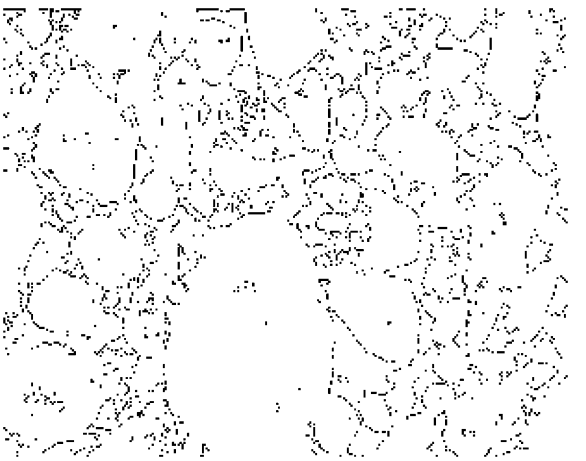

Fig. 5. Perimeter pixels related to thin section shown in Fig. 2. Each black pixel corresponds to perimeter between grey and white areas resulting from original image.

intragranular and moldic porosity. A grainstone has many perimeter pixels due to many white areas (Fig. 5), while a mudstone shows few white areas and is characterized by few perimeter pixels.

2.3.4. Number of white areas

The grey tone image is converted into a black and white image changing the grey pixels of the original image into black pixels. A labelling algorithm locates and counts the white areas. The value of the feature is the number of white areas. A grainstone has many more white areas than a mudstone.

2.3.5. Number of pixels of white areas

The value of this feature is the number of pixels that compose the white areas used to extract the previous feature.

2.3.6. Number of white areas composed of more than 150 pixels

The previous black and white image and the image resulting from the labelling are considered. The number of pixels pertaining to each white area is estimated, the feature value is the number of the white areas with more than 150 pixels (Fig. 6). This threshold has been estimated experimentally on thin sections without pronounced post-depositional features (dolomite crystals, fractures filled by sparry calcite).

2.3.7. Number of pixels within the white areas composed of more than 150 pixels

The value of this feature is the number of pixels of the white areas already used to calculate the previous feature. Mudstone and wackestone do not reveal large white areas.

2.3.8. Number of pixels of the white areas

The results of the previous labelling algorithm are considered here. The white areas are ordered according to their number of pixels. The 4 greatest white areas are chosen by estimating the number of pixels for each of them. In this way, 4 features are obtained. A wide variety of grainstones has been used to count the number of white areas in order to determine the above threshold.

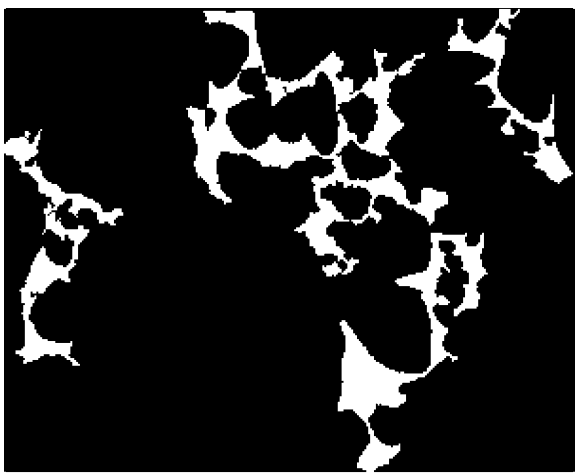

Fig. 6. Four white areas with over 150 pixels related to thin section of Fig. 2.

2.3.9. Length in pixel of the white area

The feature value for each of the previous 4 greatest white areas is the number of columns used to represent the area in the image matrix.

2.3.10. Number of small and large convex deficiencies

For each of the previous 4 white areas, the convex hull (Gonzalez, 2004; Liu-Yu and Thonnat, 1997) and the corresponding convex deficiencies are computed. A labelling algorithm locates and counts the convex deficiencies. The value of the features (j) and (k) corresponds to the number of convex deficiencies composed by less than 100 pixels and to the convex deficiencies composed of more than 1000 pixels, respectively. The values 100 and 1000 were determined by analysis of a wide variety of white areas in images of grainstone and packstone.

A white area due to intergranular calcite cement has a large convex hull, a low number of small convex deficiencies and a high number of large convex deficiencies (Fig. 7A–C). On the contrary, a white area due to intragranular calcite cement has a small convex hull, a high number of small convex deficiencies and a low number of large convex deficiencies (Fig. 7D–F).

2.4. Feature normalization

To prevent singular features from dominating the others and to obtain comparable value ranges, a linear transformation provides for all the features to have values in the range $[-1.0, 1.0]$.

2.5. Input dimension reduction

Often, the components of the input vector are highly correlated (redundant). So it is useful to reduce the dimension of the input vectors, in order to simplify the structure of the classifier and to obtain a faster training. The principal component analysis (PCA) is a linear input dimension reduction technique that computes the largest eigenvectors of the covariance matrix of the feature set (Bishop, 1998). PCA selects the most expressive features related to eigenvectors with the largest eigenvalues, so PCA approximates the feature set space by a linear subspace.

Analyzing the eigenvalues in decreasing order, 15 from the 23 extracted features, are selected as inputs.

2.6. Neural networks

Neural networks are models for expressing knowledge using a connectionist paradigm inspired by the mechanisms at work in human brain. The processing element is the neuron, by analogy with the neuron of the brain. The network is composed of many neurons

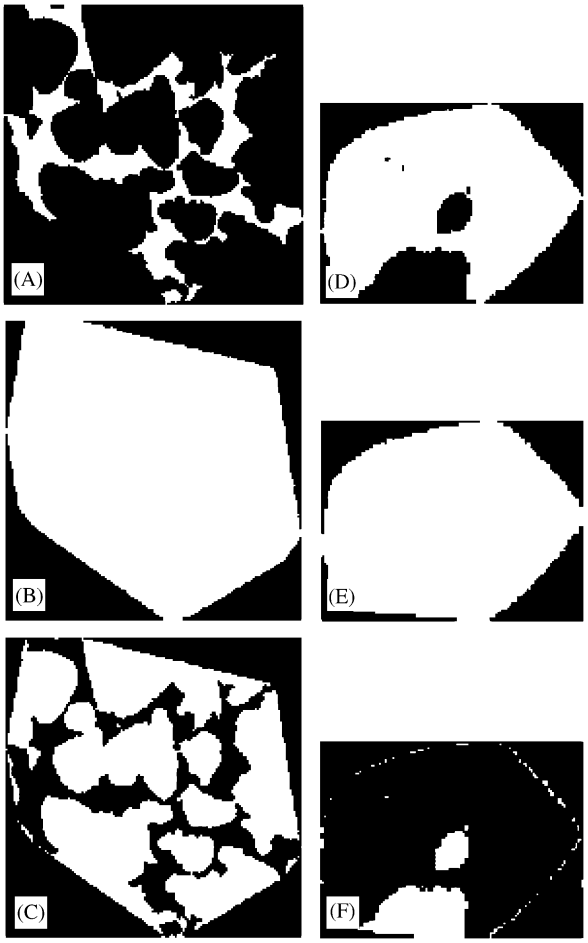

Fig. 7. (A) White areas due to intergranular calcite cement, (B) convex hull, (C) large convex deficiencies, (D) White area due to the intragranular calcite cement (microfossil chamber), (E) convex hull, (F) small convex deficiencies.

linked by a set of weighted connections. The knowledge is represented by value of the weights on connections.

To obtain the output of the neural network it is necessary to assign a value to each input neuron and to compute the corresponding equation for each neuron; the set of output values of the network is composed of the values of the output layer neurons.

Their use is recommended when:

- there is no algorithm or model to solve the problem;
- there are more data input/output operations than computations;
- many examples for supervised training are available.

All these requirements are fulfilled by the problem discussed here, thus making neural networks an ideal tool. The classification problem is the assignment of an object characterized by a set of features to one predefined class; it is a sort of mapping from a feature space to a class space, using a non-linear mapping function. A neural network can represent an arbitrary function mapping among spaces of several dimensions.

In order to design the neural network that achieves good mapping and training, according to Bishop (1998) who describes the mathematical details related to supervised neural networks, we need to choose:

1. neural network model;
2. activation function for each neuron;
3. error and minimization functions;
4. training algorithm.

2.6.1. Neural network model

We use the multi-layer perceptron neural network (MLP) because the number of output classes is fixed. An MLP is a three-layer feed-forward network. The neurons are grouped in input, output and hidden (i.e. those units which are neither input nor output) layers. Each neuron of a given layer is connected to all the neurons of the next one (Fig. 8).

According to PCA, the input layer has 15 neurons while the output layer has 4 neurons corresponding to each Dunham class; the hidden layer has 8 neurons. Other parameters configuration show less than 91.0% of correct classification.

2.6.2. Activation function for each neuron

The hidden neurons use the tanh activation function. In our MLP each output value lies in the range [0.0, 1.0] and the global sum is 1, in order to consider these values as probability of good classification. This can be achieved by using for each output neuron the softmax activation function.

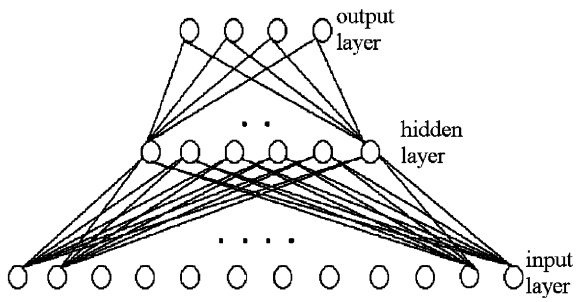

Fig. 8. MLP network used and composed of neurons: 15 input, 8 hidden, 4 output corresponding to 4 classes of Dunham classification.

2.6.3. Error and minimization functions

The MLP use cross-entropy error function and the quasi-Newton minimization error function.

2.6.4. Training algorithm

In the case of MLP, a supervised training must be used in which the network learns from a training set consisting of features input and the desired class outputs. The training procedure was the back-propagation method: we give to the input neurons the first pattern and the network gives its output. If this is not equal to the desired output pattern, then the procedure computes the difference (mean square error) between these two values and changes the weights in order to minimize them. These operations are repeated for each input pattern until the error is minimized.

In this work the weight matrix is composed of small random values. The training set was composed of 400 grey-tone images, 100 for each Dunham class from marine carbonates of different ages, localities and environments. These digitized images are taken from a set of photo collections excluding, for these experiments, more complex examples in which are documented early to late diagenetic (bioturbation, karstification, dolomitization, recrystallization and so on) processes.

We used the early stopping method to learn the mathematical model that describes statistically the feature set (generalization property). In this way the MLP can correctly classify other images not used in the training step. The MLP is tested with the validation set every 10 epochs (an epoch is a training cycle from the whole feature set). The validation set was composed of 132 images, 32 for each texture class. The training error monotonically decreases as training progresses, while the validation set error only decreases up to a certain point, after which it increases (Fig. 9). The training is stopped at the minimum of the validation error: the validation error is 0.31 and the related training error is 0.17.

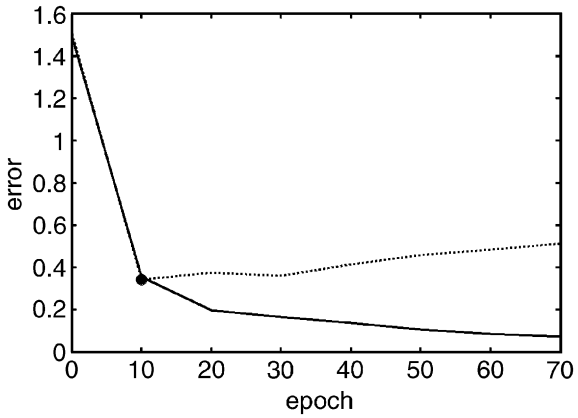

Fig. 9. Evaluation of training set and validation set errors as training progresses. Training and validation error are shown by solid and dotted lines, respectively. Minimum error for validation set is shown by black circle on dotted line. Epoch is indicated on horizontal axis.

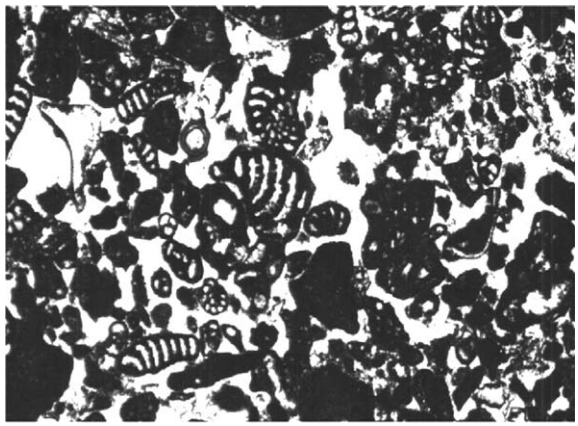

Fig. 10. Example of grainstone from test set, erroneously classified as packstone.

2.6.5. Analysis of the test set results

The test set is composed of images not used in the training and validation set, in order to estimate the final classification performance of the MLP. The first test set was composed of 268 images from personal photo collections, 67 for each Dunham class.

MLP classified 250 images correctly (93.3%) and 18 images erroneously (6.7%). For what concerns the wackestones, 4 were uncorrectly classified as packstone because they showed recrystallization to microsparry calcite and/or bioturbation. Only 1 wackestone with very small microfossils was read as mudstone because the pre-selected magnification was insufficient to identify them by means of the feature extraction. Among the grainstones, 1 image was erroneously classified as packstones, due to the presence of micritized grains often associated with intraclasts showing a mud-supported texture (Fig. 10).

The confusion matrix (Table 1) allows to summarize the classification results: the columns represent the true classes and the rows the assigned classes. In case of erroneous classification, the class chosen by the MLP is contiguous to the correct one (Fig. 11). It may be seen that it never occurs that an image of a grainstone is classified as wackestone or mudstone.

Considering only mud-supported (mudstone and wackestone) and grain-supported (packstone and grainstone) textural classes, the percentages of accuracy become 97.0% and 93.3%, respectively.

Table 1
Confusion matrix of test set from collections

Assigned	True class			
	M	W	P	G
M	65	1	0	0
W	2	62	9	0
P	0	4	57	1
G	0	0	1	66

M = mudstone, W = wackestone, P = packstone and G = grainstone.

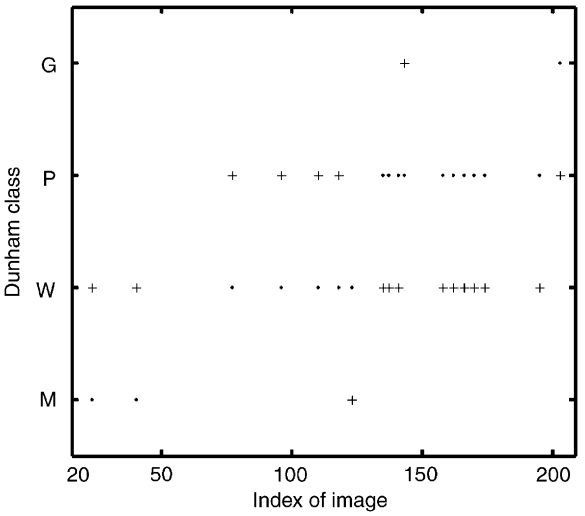

Fig. 11. For each misclassified image in test set, points show correct class and crosses indicate corresponding neural network output.

The results shown in Table 1 have been obtained using a classification strategy based on the choice of the class suggested by the highest output. It is worth noting that when the 4 output values of the MLP are very similar among them, so that the highest value is very far from 1, the MLP classifies the image with high probability of uncertainty. In this case only with a support of the sedimentologist it is possible to exactly classify the above images that are selected on the basis of the following threshold decision rule: if the highest output value is less than (or equal to) the rejection threshold, then the corresponding image has to be classified by the sedimentologist; in other case the MLP classification may be accepted.

It is important to choose an optimal value for the rejection threshold. Clearly, more images are rejected and fewer errors are made if the value of the rejection threshold is increasing. Using the output values provided by the MLP for the test set, each highest output value is compared with a rejection value in the range [0.0, 1.0].

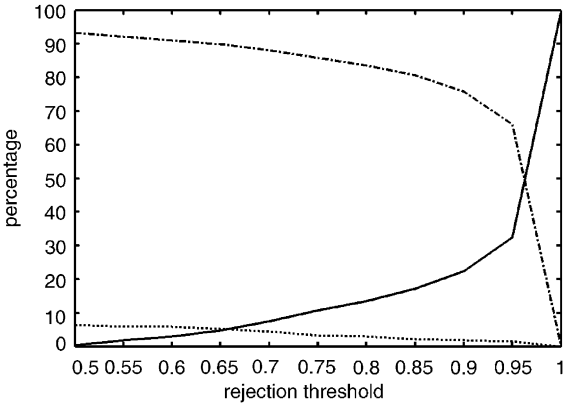

Fig. 12. Percentage of classification for each value of rejection threshold in range [0.0, 1.0]. Percentage of correct classifications is shown by dash–dot line whereas percentage of wrong classifications is shown by dotted line and percentage of uncertain classifications is shown by solid line.

From Fig. 12 it appears that the value 0.6 is the rejection threshold to make an acceptable percentage of the images classified as well, wrong or uncertain. The threshold discriminates 8 uncertain images (3.0%), 16 images wrongly classified (6.0%) and 244 images well classified (91.0%).

Another criterion used to discriminate among uncertain classifications is to calculate the difference between the first and second highest values. A difference less than 0.2 shows that the MLP is undecided between the two classes corresponding to these two values. In this case, only 7 images are discriminated to be classified by direct inspection (2.6%)

3. San Lorenzello case study

3.1. Description

The section tested in this paper is well exposed along a road cut on the southern hill-side of Monte Monaco di Gioia, (Matese Mountains) about 80 km from Naples (Italy). The San Lorenzello section, about 86 m thick, is made of shallow-water carbonate rocks of the Early Cretaceous age. It was measured and sampled at centimetre scale for sedimentological and cyclostratigraphic studies (D'Argenio et al., 1997; Ferreri et al., 2001, 2004).

Textures and sedimentary structures were sequentially collected in the field; then they were integrated with a careful analysis of about 250 thin sections. These carbonates consist of alternating grain- and mud-supported lagoonal to peritidal sediments with benthic foraminifera, and/or green algae, and/or molluscan shells (Fig. 13).

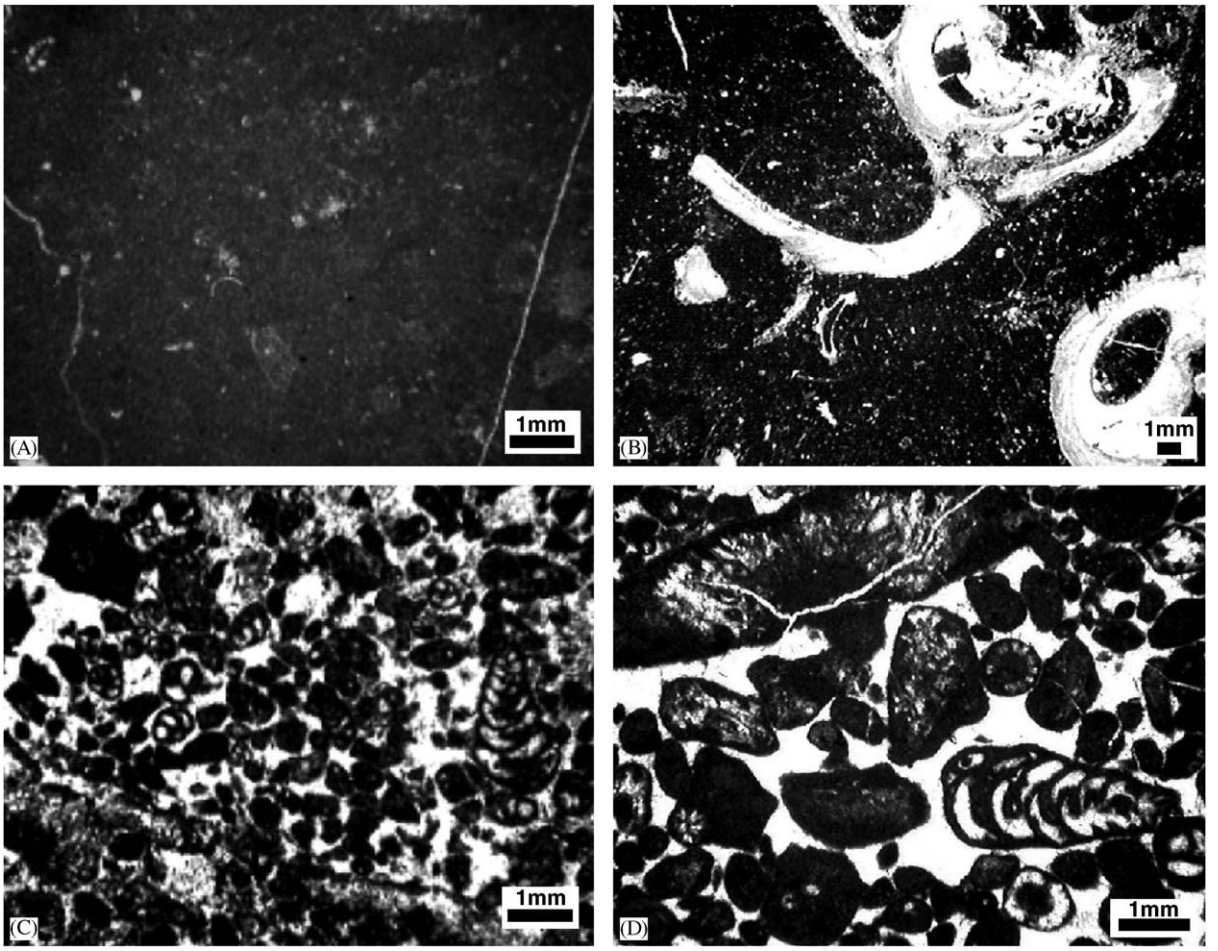

Fig. 13. San Lorenzello shallow-water carbonate deposits. Example of textures acquired by digital camera: (A) mudstone with oligotypic fauna represented by ostracods and rare small benthic forams; (B) wackestone with molluscan shells, green algae and benthic forams; (C) fine packstone with benthic forams, peloids and rare small intraclasts; (D) grainstone with bioclasts (green algae, benthic forams, molluscs), intraclasts, micritized grains and peloids.

This test set of 215 thin sections includes: 22 mudstones (10.2% of the set), 100 wackestones (46.5%), 67 packstones (31.1%) and 26 grainstones (12.2%). In the above 4 Dunham classes all the transitional textures (as mudstone–wackestone, wackestone–packstone and packstone–grainstone) have been included, based on their prevailing ($\geqslant$70%) estimated texture. About 35 thin sections were excluded from the test set because the original texture resulted, obliterated by superimposed diagenesis (dolomitization and/or karst) that has not been considered in the present work. We could correlate to each other the results obtained using two different methodological approaches: manual and automatic.

3.2. Results and discussion

The second test set has been identified by the proposed automatic methodology. It has been possible to predict with 93.5% accuracy the type of texture, this means that 201 of the 215 images have been exactly determined by MLP.

Table 2
Confusion matrix of San Lorenzello case study

Assigned	True class			
	M	W	P	G
M	22	0	0	0
W	0	98	10	0
P	0	2	57	2
G	0	0	0	24

For key letters see caption of Table 1.

Table 2 shows the confusion matrix. All the digitized images with values of texture less than 0.6 have been

checked in order to understand the peculiar result. In fact, many sedimentological parameters can complicate the original depositional signal, at the moment not acquired by our technique. Microsparite and/or dolomite crystals have been recognized in the matrix of some wackestones; these diagenetic characteristics attribute higher values to the packstone fraction, if we compare these examples of wackestones with those without these diagenetic modifications. For instance, a small number of well-defined crystals that derive from post-depositional dolomitization of mudstones has been identified by feature extraction as grains, increasing the values of the grain-supported fraction.

On the other hand, micritization, small size and densely packed grains in some packstones are other complex characteristics that our neural network, at present, is unable to individuate. As a consequence, fine packstones appear to have higher mud-supported fraction and may be viewed as wackestones. In fact, 10 images identified as wackestones, are instead packstones, because minor thickness variation in the thin sections may influence brightness and contrast of the images. Moreover, intraclasts and peloids, very frequent in these packstones, may be recognized as "mud". As a consequence, contrast between grains (especially peloids) and sedimentary matrix not always results clearly and even if the contrast is increased, the different grey level values may not be individuated during the features extraction. Grains must have a well-defined internal structure and a clear boundary, so that grey level values have tones in contrast with those of the matrix. Only under these conditions may all packstones be exactly determined by the neural network.

Mud-supported textures have been more exactly identified (98.4% accuracy) than grain-supported textures (89.2% accuracy) and only 12 images resulted misclassified.

As discussed above, the accuracy of the texture identification depends on the difference between the two highest numerical values. A difference less than 0.2 means that the technique recognizes, on the whole, a mixture of the two textures. Seven images have revealed a difference less than 0.2. In nature, there are examples of transitional textures as packstone–wackestone or wackestone–mudstone and so on, qualitatively revealed by the human eye.

4. Conclusions

In this paper we have proposed a new numerical approach based on image processing and multi-layer perceptron neural network that allowed us to classify carbonate rocks by grey level images digitized from thin sections, using the Dunham textural classification. This technique predicts the type of texture from the digitized images of thin sections with 93.3% and 93.5% accuracy on two test sets of 268 and 215 images, respectively. This percentage is satisfactory for this preliminary application of the proposed methodology. In the future, larger training and test sets on different carbonate rocks of origin and age could provide further improvements.

Techniques for image processing must be chosen carefully and adapted to the optical characteristics of each specific collection of thin sections. Moreover, at present, there is no standard system for image processing of thin sections, because there are some difficulties that may be circumvented by using higher resolution and/or magnification during the image acquisition.

At present, our preliminary results are encouraging and indicate that a good choice of features and a specific neural network can make, in a rapid and accurate way, a good automatic textural classification. Moreover, in the future it appears possible to expand the number of textural classes, also considering the transitional ones as well as thin sections showing sin- and post-depositional diagenetic modifications (microsparitization, karstification, dolomitization and so on), so that the tested methodology could be carried out on all types of carbonate rocks. To conclude, the present results indicate another useful application of neural networks to the geosciences.

Acknowledgements

Financial and technical support was provided by Dipartimento di Scienze della Terra, Università Federico II, Naples; IAMC, Istituto per l'Ambiente Marino Costiero, CNR, Naples and Istituto Nazionale Fisica della Materia, Università di Salerno. We wish to thank Bruno D'Argenio for helpful and constructive comments during the manuscript preparation and John Doveton and an anonymous reviewer for their useful suggestions during the submitting process. Finally, we are also grateful to Patricia Sclafani and Tom Hopkins who contributed to improve our English language quality.

References

Bishop, C.M., 1998. Neural Networks for Pattern Recognition. Clarendon Press, Oxford 256pp.

Chang, H.-C., Kopaska-Merkel, D.C., Chen, H.-C., 2002. Identification of lithofacies using Kohonen self-organizing maps. Computers & Geosciences 28 (2), 223–229.

D'Argenio, B., Ferreri, V., Amodio, S., Pelosi, N., 1997. Hierarchy of high-frequency cycles and time calibration in Cretaceous carbonate platform strata. Sedimentary Geology 113, 169–193.

Dunham, R.J., 1962. Classification of carbonate rocks according to depositional texture. In: Ham, W.E. (Ed.), Classification of Carbonate Rocks. American Association of Petroleum Geologists, Memoir 1, Tulsa, OK, pp. 108–121.

Ferreri, V., Amodio, S., D'Argenio, B., Sandulli, R., 2001. High-resolution correlation and orbital chronostratigraphy at the Valanginian–Hauterivian boundary. Society of Economic Paleontologists and Mineralogists International Workshop, Sorrento, Italy, Abstract Volume, pp. 27–28.

Ferreri, V., Amodio, S., Sandulli, R., D'Argenio, B., 2004. Orbital chronostratigraphy at the Valanginian/Hauterivian boundary. A cyclostratigraphic approach. In: D'Argenio, B., Fischer, A.G., Premoli Silva, I., Weissert, H., Ferreri, V. (Eds.), Cyclostratigraphy: Approaches and Case Histories. Society of Economic Paleontologists and Mineralogists Special Publication 81, Tulsa, OK, pp. 153–166.

Gonzalez, R.C., 2004. Digital Image Analysis Using MATLAB. Pearson Prentice-Hall, Upper Saddle River, NJ 609pp.

Liu-Yu, S., Thonnat, M., 1997. Description of object shapes by apparent boundary and convex hull. Pattern Recognition 26, 107–195.

Nabney, I.T., 2002. NETLAB Algorithms for Pattern Recognition. Springer, Berlin 420pp.

Shapiro, L., Haralick, R., 1993. Computer and Robot Vision. Addison-Wesley Publishing Company, Reading, MA vol. 1, 630pp. and vol. 2, 672pp.

Tagliaferri, R., Longo, G., D'Argenio, B., Incoronato, A. (Eds.), 2003. Neural network: analysis of complex scientific data. Neural Networks 16(3/4), 295–517.

Tucker, M.E., Wright, V.P., 1990. Carbonate Sedimentology. Blackwell Scientific Publications, Oxford 481pp.